Resource allocation in 5G multi-tenancy network slicing for balancing distribution power systems

Vajiheh Farhadi[1], Thomas La Porta[2], Ting He[3], Nilanjan Ray Chaudhuri[4],

Pennsylvania State University,
{[1]vuf8,[2]tfl12,[3]tzh58,[4]nuc88}@psu.edu

***Abstract*—In recent years consumers of power have also started to generate power via renewable sources such as wind and solar. In smart grid distribution systems controls are applied to regulate the consumption and distribution of energy to save energy and costs. These controls rely on monitoring of the power distribution system. To monitor these system sufficiently to optimize power flow can be costly. The advent of fifth generation (5G) networks presents an opportunity to improve monitoring capabilities at low cost. In the 5th generation of mobile cellular networks, end-to-end network slicing is the critical enabler, such that an infrastructure provider creates various network slices for different Mobile Virtual Network Operators (MVNOs) to accommodate various services. This work assumes each MVNO is a power company while nodes are sensors and actuators in the power grid. Proper resource allocation for numerous coexisting network slices is vital. We address this issue by proposing a novel scheme in Radio Access Network (RAN) network slicing to maximize spectral efficiency, subject to guaranteeing each sensor and actuator in the power grid receive a minimum requirement of slices. We characterize the fundamental hardness of our problem and develop a greedy heuristic. Next, via simulations on the IEEE 13-, 34- and 37-node test feeders, we show that the proposed algorithm achieves superior performance in terms of served power after balancing the unbalanced distributed power system.**

***Index Terms*—5G, network slicing, SCADA system, distribution power system, unbalanced system**

I. Background & Related work

A smart power grid is a modernized power grid that uses information and communication technologies to collect information and dispatch control commands to the power grid. This information is used to remotely regulate the production and distribution of electricity or adjust power consumption to save energy and reduce losses. In a distribution power system where consumers also generate energy through distributed generators, the power flow must be balanced continually and quickly. To do that, there must be robust monitoring which can be very costly. We propose using 5G technology to enable this monitoring and control with sufficient performance and connectivity in a cost-effective manner.

The United Nation estimates that up to 85 percent of electricity must be renewable by 2050 to combat the effects of climate change [1]. Consequently, house owners are inspired to install solar panels, wind turbines, or other energy-generating sources due to their low carbon emissions [1]. Moving toward solar and wind energy leads to an increased risk of network disturbances, such as overvoltage, harmonics distortion, reverse power flows, or power losses [2], which requires faster responses to adjust the balance between generation and consumption. Therefore, connectivity of power grid components to control networks such as Supervisory Control and Data Acquisition (SCADA) system plays a critical role.

Authors in [3] claim that 95% of blackouts occur in the last 5-kilometers of the power grid, i.e. the distribution and consumption part, which is the major bottleneck for smart grid development. This is because of low coverage due to the distribution pattern and the tremendous number of users, especially in dense urban areas [4]. Operating optical fiber in these areas is costly and has deployment difficulties; however, the new emerging 5G technology effectively addresses this problem.

Recently, due to the growing usage of distributed energy resources such as solar PhotoVoltaic (PV), distribution networks need to be actively supervised to guarantee their reliability and optimized operation. The Optimal Power Flow is one of the methods to do so, which provides solutions for switching optimization, transformer tap optimization, Conservation Voltage Reduction (CVR), or Volt/VAR Optimization (VVO) [5].

As an appropriate means of "going to meet the objectives of transitioning to this next-gen grid" [6], 5G offers reduced maintenance and lower CapEx investment in grid communication infrastructure, which is facilitated by relaxing the need for extensive fiber optic cabling. In general, the applications of smart grids are categorized as intelligent distributed feeder automation, millisecond-level precise load control, information acquirement of low voltage distribution systems, and distributed power supplies [3], [4]. Table I shows network requirement of these applications [4]. As 5G network slicing satisfies all these demands, this work focuses on the appropriate allocation of network bandwidth to different slices, such that appropriate connectivity of the power grid's component is provided and the requirement of different slices are ensured.

The primary innovation in 5G is virtualization, such that instead of dedicated physical servers, network functions represent network elements. Network function virtualization enables network slicing, which allows operators to divide the network into virtual slices such that all run on shared physical infrastructure. Each slice is a virtual, end-to-end individual, and logical network of its own, while all components that represent communication, such as data speed, privacy, or latency can be customized in each slice by a customer use case. Each user

This work was supported by the National Science Foundation under award ECCS-1836827.

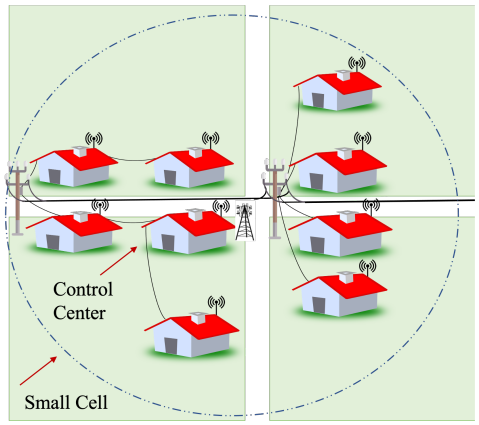

Figure 1: distribution system where homes/lines are nodes (V)/transmission lines (E)

can simultaneously support one or more slices, depending on the functionality it implements [7].

Each network slice contains RAN slice, core slice, and transport slice which is the connectivity between RAN and core slices. In this paper, we solely focus on slicing the RAN in 5G-NR. The main idea of RAN slicing resource allocation is optimizing the performance of the entire network system while ensuring the various users' requirements. 5G-NR has been designed to support various verticals having a wide range of requirements. Also, 5G-NR defines different numerologies (or subcarrier spacing) [8]. However, due to its complexity, most of the works only use the same numerology throughout the network slice life-time [8]–[11], which is the same method in this paper. Research on multiple numerologies and core network slicing is left to future works.

Resource allocation of network slicing plays a crucial role in resource utilization and networking performance. It is realized as centralized versus hierarchical schemes. In the former approach, the infrastructure provider allocates the resource to users, which creates a huge computational overhead. However, in hierarchical schemes different entities such as Mobile Virtual Network Operators (MVNO) are involved and the resources owned by an infrastructure provider are shared by multiple MVNOs [12]. In this work, we focus on bandwidth allocation from the perspective of a layer between physical and slice, i.e., MVNO, and assume each MVNO represents a power company, while users are sensors and actuators in the power grid.

Summary of Contributions

Table I: The communication network requirement for (i) intelligent distributed feeder automation, (ii) millisecond-level precise load control, (iii) information acquirement of low voltage distribution systems, and (iv) distributed power supplies.

	Latency req. (milliseconds)	Reliability req. (99.999%)	Users' density req. (millions to tens of millions)
(i)	High	High	High
(ii)	High	High	High
(iii)	Low	Medium	Low
(iv)	High	High	Medium

Our contributions in this paper include:

1) We consider a SCADA communication network for the distribution power grid and assume that all communication links are network slices. We posed as an optimization of maximizing the total power demand served by assigning appropriate slices as a communication medium between the CC and sensors/actuators in the distribution power grid.

2) As the total served power is not an explicit function of the decision variables, we propose a proxy objective function capturing the observability/controllability of nodes in the grid, weighted by their importance in the system topology and the their service. The solution is a set of assigned slices to nodes in the power grid. The number and type of slices are limited by the network bandwidth.

3) We formulate the underlying optimization as a non-linear problem, which is proved to be NP-hard. The problem maximizes spectral efficiency, subject to providing nodes in the power grid a guaranteed delay and connectivity requirements.

4) We apply greedy heuristic and by performing extensive evaluations on the IEEE 13-, 34- and 37-node test feeders, we show that the proposed heuristic outperforms baselines.

A. *Related Work*

Resource allocation and network slicing in RAN and their challenges are popular discussed topics in the literature. Nowadays, with the emergence of new 5G various services, the concept of network slicing is gaining notable importance. Authors in [13], [14] provide a survey on resource allocation challenges and the enabling technologies in network slicing. Literature [15]–[22] focus on sharing radio resources for satisfying different coexisted 5G services simultaneously. 5G accommodates four major usage scenarios namely, Enhanced Mobile Broadband (eMBB), Ultra-reliable Low-Latency Communications (URLLC), Massive Machine-Type Communications (mMTC) and vehicle-to-X (v2x) communications, in detail [23], [24]. Here is a brief summary of them: 1) eMBB, where these applications are very video-centric, consume much bandwidth, and generate the most traffic on the mobile network. Here, the peak data rate reaches as much as 20 gigabits per second in downlink and 10 gigabits per second in uplink; 2) URLLC, which accommodate applications where both extra reliability and low latency are demanded, such as remote surgery or millisecond-level load controls in smart grids. The Radio Access Network (RAN) delivers less than one-millisecond service latencies in this slice type; 3) mMTC, or the massive internet of things device (mIoT), where the connection density is very high; however, these devices generate far less traffic than eMBB applications; 4) v2x communications, which allows the communication between vehicles with other infrastructure (vehicle-to-infrastructure) and other vehicles (vehicle-to-vehicle) around them for improved transport fluidity, safety, and comfort on the road.

Literature [15], [18] propose an optimal joint scheduler on a two timescale framework of slot and minislot, with the dual objectives of maximizing utility for eMBB traffic while immediately satisfying URLLC demands. eMBB resource

allocations occur at slot boundaries, whereas URLLC traffic is pre-emptively overlapped at the minislot timescale to reduce latency. In [16], the authors allocate resources to the incoming URLLC traffic while minimizing the risk of the eMBB transmission (i.e., protecting the eMBB users with low data rate) and ensuring URLLC reliability. They consider the Conditional Value at Risk (CVaR) as a risk measure for eMBB transmission. Literature [17] introduces the optimization problem of maximizing the eMBB data rate subject to URLLC reliability constraint, while considering the variance of the eMBB data rate to reduce the impact of immediately scheduled URLLC traffic on the eMBB reliability. Literature [21] studies the heterogeneous nonorthogonal multiple access sharing of RAN resources in uplink communications from a set of eMBB, mMTC, and URLLC devices to a common base station. They assume that users have homogeneous requirements. Literature [22] proposes an End-to-End Slicing as a Service framework for eMBB, URLLC, and mMTC applications.

The concepts of network sharing and multi-tenancy were described in [22], [25], [26], where infrastructure provider deploys 5G network and mobile network operators lease the slices from infrastructure provider to serve their end-users.

Roadmap: The remainder of the paper is organized as follows. Section II shows models of optimal power flow and communication network in a coupled system of the power grid and communication network. Section III formulates the optimization problem and analyzes the complexity. Next, it presents the proposed heuristic algorithm. Section IV evaluates the performance of the proposed solution against benchmarks. Finally, section V concludes the paper.

II. System Model

This paper studies a coupled power grid with a geographically co-located SCADA-based communication network. A Control Center (CC) gathers data from sensors/actuators and dispatches control commands to generators, loads, and switches.

This section provides specifics of the optimal power flow model in the distribution power grid and communication network.

A. Modeling Optimal Power Flow

A distribution power grid $G(V, E)$ is composed of buses and transmission lines connecting the buses. There is a substation source bus with a fixed voltage. Each line $(i, j) \in E$ connects bus $i \in V$ to bus $j \in V$ such that i is on the path between the substation source bus and j. Fig. 3 shows different distribution power grids where the dots and lines indicate set of buses (V) and transmission lines (E), respectively. The substation source buses, are the buses with solid line (i,e,. 650, 800, 799).
Fig.1 depicts a distribution power grid where the homes and lines are buses (V) and transmission lines (E), respectively.

Power flows in power systems are governed by three laws, Ohm's, current balance and power balance [27]. Optimal power flow determines the power injection that minimizes total generation cost, subject to physical and operational constraints. In general, optimal power flow problems in distribution networks are non-linear and non-convex due to their specific characteristics [28]. Distribution systems are usually multiphase and radial, the three phases are usually unbalanced, and loads cannot be modeled independently of the voltage [29]. In this paper, we use the technique in [30], where the authors introduce semidefinite programming models to solve optimal power flow problem in distribution systems. It is formulated as problem (1) on two-phase or single-phase laterals and problem (2) on the three-phase backbones [30].

$$\min \sum_{i \in V} \text{Cost}_i(n_i) \tag{1a}$$

$$\text{s.t.} \sum_{i:(i,j)} diag(S_{ij} - z_{ij} I_{ij}) + s_j + x_j v_j = \sum_{k:(j,k)} diag(S_{jk})^{\phi_j},\ j \in V \tag{1b}$$

$$v_j = v_i^{\phi_{ij}} - (S_{ij} z_{ij}^H + S_{ij}^H z_{ij}) + z_{ij} l_{ij} z_{ij}^H,\ (i,j) \in E \tag{1c}$$

$$v_i \le diag(v_i) \le \bar{v_i},\ i \in V \tag{1d}$$

$$v_0 = V_0^{src} (V_0^{src})^H \tag{1e}$$

$$\begin{bmatrix} v_i^{\phi_{ij}} & S_{ij} \\ S_{ij}^H & l_{ij} \end{bmatrix} \ge 0, (i,j) \in E \tag{1f}$$

$$\min \sum_{i \in V} \text{Cost}_i(n_i) \tag{2a}$$

$$\text{s.t.} \sum_{i:(i,j)} diag(M(S_{ij}^{012} - z_{ij}^{012} L_{ij}^{012}) M^H) + s_j + x_j^{012} v_j^{012} = \sum_{k:(j,k)} diag(M S_{jk}^{012} M^H) \tag{2b}$$

$$v_j^{012} = v_i^{012} - (S_{ij}^{012} z_{ij}^{012,H} + S_{ij}^{012,H} z_{ij}^{012}) + z_{ij}^{012} l_{ij}^{012} z_{ij}^{012,H} \tag{2c}$$

$$v_i \le diag(M v_i^{012} M^H) \le \bar{v_i},\ i \in V \tag{2d}$$

$$v_0^{012} = V_0^{012,src} (V_0^{012,src})^H \tag{2e}$$

$$\begin{bmatrix} v_i^{012} & S_{ij}^{012} \\ S_{ij}^{012,H} & l_{ij}^{012} \end{bmatrix} \ge 0,\ (i,j) \in E \tag{2f}$$

Here, $v_i = V_i V_i^H$, $l_{ij} = I_{ij} I_{ij}^H$ and $S_{ij} = V_i^{\phi_{ij}} I_{ij}^H$, where H indicates the Hermitian transpose. $V_i = V_I^{ab} = [V_i^a, V_i^b]^T$ (assuming node i has two phases a, b) and L_{ij} vectors define the nodal voltage of bus i and line (i, j), respectively, and ϕ_i and ϕ_{ij} denote their phases. If the power system is on the three-phase laterals, voltages in phase components are transformed into symmetrical components as $V^{abc} = MV^{012}$, such that M is a normalized 3×3 matrix and $M^H = M^{-1}$.

Objective functions (1a) and (2a) minimize the total generation cost of the power grid, where Cost_i is the generation cost of node i and $n_i \in \mathbf{C}^{|\phi_i|}$ is the nodal injection at node i. Constraints (1b) and (2b) impose the power flow balance for each bus, while constraints (1c) and (2c) demonstrate Kirchoff's voltage law along each line. (1d) and (2d) enforce the bounds on the nodal voltage, and constraints (1e) and (2e) set the voltage at the substation source bus. (1f)

and (2f) are the positive semidefinite constraints.

The CC houses the control center in the SCADA-based communication network and has updated information of the elements in the power grid which are connected to them through slices. Based on the power grid information, it determines the power injection of all buses by solving the optimal power flow problem (1) or (2).

B. Communication Network & Network Slicing

The dominant trend in 5G deployment is small cell base stations. Each small cell consists of small low-power antennas and are always connected by fiber optic cable attached to the infrastructure like street lights, utility poles, or slimline poles [4].

To control the interference between small cells, we use the Fractional Frequency Reuse (FFR) technique [41]. In FFR, the coverage area in each cell is divided into inner and outer zones. Every cell transmits in the same frequency in the inner zone (which allocates the major part of the resources), while the outer zones uses different resources to reduce interference. In this work, we use the homogeneous small cells deployment with FFR technique, as shown in Fig. 2. In this context, we use words 'small cell' and 'cell' interchangeably.

Based on the various requirement of the smart grid, discussed in Table. I, we consider two different slices: mMTC slice for monitoring purposes, which is required in uplink direction; and URLLC slice for controlling purpose, which is needed in downlink direction. A centralized CC is connected to all gNBs. The CC receives/sends information to/from any node if it is connected to that particular node through mMTC/URLLC slice.

Orthogonal Frequency Division Multiple Access (OFDMA) is used as the multiple access in this work. Note that we only consider one numerology (subcarrier spacing) here. OFDMA is commonly used in 5G [9]–[11] due to its powerful performance in dealing with multipath signals and compatibility with multi-input multi-output (MIMO) antennas. In OFDMA, the bandwidth is divided into small divisions called physical resource blocks where each physical resource block is 180 kHz and has 12 adjacent OFDM subcarriers [32]. The single physical resource block is allocated to a single device for at least a single transmission time interval that is equal to 1 ms [32].

The infrastructure provider allocates resource blocks to each MVNO $m \in M$ based on its service level agreement (SLA) which determines number of required resource blocks and is not less than $\kappa_m|N|$. Here, κ_m is the pre-agreed access ratio between infrastructure provider and MVNO m, such that $\sum_{m\in M} \kappa_m \leq 1$.

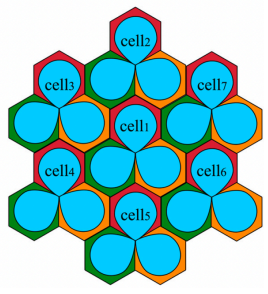

Figure 2: Network model showing FFR frequency assignment for different small cells. In each small cell, the blue is the part of the bandwidth assigned to the inner zone, while the colored parts are for outer zones [31]

Our analysis implements a constant transmission power P for all gNBs for inner and outer zones in the coverage area of gNB. Moreover, we assume all communication nodes have battery backups, and there is no power limitation for uplink transmitting.

The proxy objective maximizes spectral efficiency of the network, which requires rate calculation. Suppose that $PL_v,\ \forall v \in V$ is the the total path loss between the serving gNB and node v in a cellular network, which considers both the distance-dependent macroscopic and the shadow fading path loss components. The macroscopic path loss is given by [11]:

$$L_{db} = 40(1 - 4 \times 10^{-3}h)\log_{10}(d/1000) - 18\log_{10}(h) + 21\log_{10}(f_c) + 80,\ (DB) \tag{3}$$

where h, d and f_c are the gNB antenna height (m), the distance between gNB and node v (m), and the carrier frequency (MHz), respectively. The shadow fading path loss component is assumed to be a Gaussian random variable with zero mean and σ standard deviation (dB). Considering X_v the log-normal shadow fading path loss of node v, hence the total path loss (PL_v) and the linear gain (G_v) between gNB and node v are [11]:

$$PL_v = L_{db} + \log_{10}(X_v),\ (DB) \tag{4}$$

$$G_v = 10^{-PL_v/10}.) \tag{5}$$

The maximum achievable rate has an upper theoretical bound represented by the well-known Shannon formula:

$$r_u \leq c = B\log_2(1 + \frac{PG_v}{N + I}). \tag{6}$$

Here, B is the allocated bandwidth, N and I denote the thermal noise power and interference. As we use FFR technique, we ignore interference part I.

Main notations used in this paper are described in Table II.

III. Problem Formulation

A. Underlying Optimization Problem

A SCADA-based system cannot work adequately without a properly designed communication network. The main improvement of this paper is providing sufficient observability and controllability over distribution power grids.

Although power flow problems aim to maximize the total power served after balancing the unbalanced system, this objective function is not an explicit function of our decision variables. To address this challenge, we propose using a proxy objective function as follows.

Suppose the owner of infrastructure provider divides network bandwidth into $|N|$ resource blocks. We have T slots for scheduling; hence, $T \times |N|$ resource blocks are available to allocate in total. We formulate our problem as (7) for each time-slot $t \in T$, each cell and each MVNO $m \in M$ which is shown in below:

$$\max \frac{1}{|N|} \sum_{v\in V} \beta_v \sum_{s\in S} \alpha_s \sum_{n\in N} x_v^{sn} r_v^{sn} \tag{7a}$$

$$\text{s.t.} \sum_{v\in V} \sum_{s\in S} a_v^s x_v^{sn} \leq 1,\ \forall n \in N \tag{7b}$$

$$\sum_{v\in V} \sum_{s\in S} \sum_{n\in N} x_v^{sn} \leq \kappa_m |N| \tag{7c}$$

$$\sum_{v\in V} \sum_{n\in N} x_v^{sn}\, P \leq P_{max},\ \forall s \in s_U \tag{7d}$$

$$x_v^{sn} \leq 0,\ \forall v \in V, s \in S, n \notin \theta_v \tag{7e}$$

$$P_r\{D_v^s \geq D_{max}^s\} \leq \epsilon,\ \forall v \in V, s \in s_U \tag{7f}$$

$$x_v^{sn} \in \{0,1\},\ \forall v \in V, s \in S, n \in N \tag{7g}$$

Here, $S = \{s_M, s_U\}$ is the set of sets of all possible slices, mMTC and URLLC, respectively. V indicates set of all nodes in the power grid. The objective function (7a) provides the maximum spectral efficiency through the allocation of the available resources to nodes. α_s shows the priority of slice $s \in S$. Furthermore, as some nodes are more critical in the power grid, we prioritize nodes by parameter β_v. Both α_s and β_v are normalized values. The binary variable x_v^{sn} indicates that a particular MVNO in a particular cell assigns resource block n to node v to provide requirement of slice s, where r_v^{sn} indicates the maximum achievable rate. Main notations are described in Table II.

To avoid interference, each resource block is assigned to only one node at each timeslot of scheduling. This is guaranteed by constraint (7b). Parameter $a_v^s = 1$ shows that node v needs slice s; otherwise it is 0. Constraint (7c) makes sure that the total number of assigned resource blocks to nodes by MVNO m is not exceeded. Because of the limited transmit power of gNB, the allocated power of all nodes is subjected to constraint (7d), where P_{max} is the maximum transmission power of gNB. Constraints (7e) imposes the FFR technique. Because there is no mobility in the power grid, all nodes in the same zone share the same range of frequency depending on their location. Here, θ_v indicates set of resource blocks associated to the zone which node v is located. Constraint (7f) guarantees the delay of node v for URLLC slice. The corresponding delay outage probability is given by [9]:

$$P_r\{D_v^s \geq D_{max}^s\} = e^{-(\sum_{n\in N} x_v^{sn} r_v^{sn} - \lambda_{max}^v) D_{max}^s} \\ ,\forall v \in V, s \in s_U \tag{8}$$

where D_v^s and D_{max}^s are the delay of node v and the maximum tolerable delay for slice s, respectively. λ_{max}^v is the data arrival rate of packets in the URLLC slice from the CC to node v. We assume the downlink queue for the URLLC slice for node v is an M/M/1 queue.

Problem (7) is non-linear integer programming. Regular non-linear or integer optimization techniques can not be applied in such a formulation since the integer decision variables lie within the log function in the objective function (7a).

Table II: Table of notations

Notation	meaning
V_i	nodal voltage of bus i
l_{ij}	nodal voltage of line (i,j)
Cost_i	generation cost of node i
n_i	nodal injection at node i
0	index of substation bus
z_{ij}	impedance of line (i,j)
x_j	nodal shunt capacitance
M	Set of MVNOs
$S = \{s_U, s_M\}$	Set of sets of URLLC slices and mMTC slices
N	Set of resource blocks
V	set of nodes (users) in power grid
x_v^{sn}	Binary variable, 1 if the corresponding MVNO assigns resource block n to node v in order to provide the requirement of slice s
a_v^s	binary parameter, 1 if node v needs slice s
θ_v	set of resource blocks associated to the zone which node v is located
κ_m	access ratio between infrastructure provider and MVNO m
P	Transmission power of gNB to a particular node
P_{max}	Maximum transmission power of gNB for each MVNO
α_s	Priority of slice s
β_v	Priority of node v
D_s^{max}	maximum tolerable delay for slice $s \in S$

B. Complexity analysis

We look at a special case of our general problem by making some assumptions: (i) κ_m, the access ratio between infrastructure provider and MVNOs are equal to 1 and $|N|$ is large enough to be unconstrained; thus constraint (7c) is unnecessary. (ii) All required slices are URLLC type and all nodes require URLLC slice, hence $a_v^{s_M} = 0, a_v^{s_U} = 1,\ \forall v \in V$. (iii) We stretch the boundary of the inner zone to the edge of the cell edge and assign all resources to the inner zone; hence, equation (7e) is relaxed. (iv) $D_{max}^s = \infty$; thus constraint (7f) is no longer needed. (v) $\alpha_s = 1$ and $\beta_v = 1$ for all slices and nodes, respectively. Therefore, problem (7) changes to problem (9):

$$\max \frac{1}{|N|} \sum_{v\in V} \sum_{n\in N} x_v^{sn} r_v^{sn} \tag{9a}$$

$$\text{s.t.} \sum_{v\in V} x_v^{sn} \leq 1,\ \forall n \in N \tag{9b}$$

$$\sum_{v\in V} \sum_{n\in N} x_v^{sn}\, P \leq P_{max}, \tag{9c}$$

$$x_v^{sn} \in \{0,1\},\ \forall v \in V, s \in s_U, n \in N \tag{9d}$$

Theorem 1. *Problem* (9) *is NP-hard.*

Proof. We prove the NP-hardness of (9) by a reduction from

0-1 knapsack problem: given a set of $\mathcal{I}$ items, each with value $\mathcal{V}_i$ and weight $\mathcal{W}_i$ $(i = 1, ..., \mathcal{I})$, select subset $\mathcal{S}$ of items such that $\sum_{i \in \mathcal{S}} \mathcal{V}_i$ is maximized while $\mathcal{W}_i \leq \Omega$, for a given size Ω of the knapsack.

Construction: For each item i, construct a resource block n, which is given by the particular MVNO to node v in order to satisfy requirement of slice s. For this item, fix the value and cost equal to $\frac{r_v^{sn}}{|N|}$ and P, respectively, and let $\Omega = P_{max}$.

Claim: The optimal solution of (9) gives the optimal solution to 0-1 knapsack problem.

Proof of the claim: The optimal solution of (9) assigns each resource block to at most one node in order to serve the requirement of the requested slice. Therefore, the assignment decision is to simply assign resource block $n \in N$ to node $v \in V$ to satisfy requirement of slice $s \in s_U$ if $x_v^{sn} = 1$; or, assign nothing if $x_v^{sn} = 0$. Let $\mathcal{S}$ be the set of indices of all assigned resource blocks to nodes under the optimal solution to (9). Then, the total throughput rate equals $\sum_{i \in \mathcal{S}} \mathcal{V}_i$, and $\sum_{i \in \mathcal{S}} \mathcal{W}_i \leq \Omega = P_{max}$. Selecting all items corresponding to the combination of nodes and resource blocks assigned by the optimal solution of (9) provides the optimal solution to 0-1 knapsack problem. □

Remark: Proving NP-hardness for the special case shows that the problem is NP-hard in the general case as well.

We now develop efficient algorithms for general problem (7).

C. Heuristic Algorithm

We propose greedy heuristic in Algorithm 1 of the general problem (7). Here, $|x_v^{sn}|_k = \{x_v^{sn_1}, ..., x_v^{sn_k}\}$ indicates assignment of k resource blocks to node v in order to satisfy requirement of slice s.

Algorithm 1: Greedy Heuristic

Input: Input parameters of (7)

Output: Resource blocks assignment to nodes for different slices x_v^{sn}

for each node and each demanded slice, calculate k, minimum number of required resource blocks to satisfy requirement of needed slices

$S \leftarrow \emptyset$;

while $\exists\ n \in N \setminus S$ such that $S \cup |x_v^{sn}|_k$ satisfies (7b)-(7f) and $N \setminus S \geq k$ **do**

$S^* \leftarrow \arg\max_{|x_v^{sn}|_k:\ S \cup |x_v^{sn}|_k \text{satisfies (7b)-(7f)}}$ objective (7a) under assignment of $(S \cup |x_v^{sn}|_k)$;

$S \leftarrow S \cup S^*$;

Convert S to x_v^{sn};

IV. Performance Evaluation

This section demonstrates performance of the proposed algorithm on different distribution electric power test systems.

A. Benchmarks and metrics

To assess performance of the proposed algorithm, we use the following benchmarks:

1) *the greedy Algorithm 1*;

2) *the BC method*, Given power grid topology $G(V, E)$, this benchmark sequentially considers the betweenness centrality of the nodes, which is the frequency that a node appears on the shortest paths between all pairs of nodes in the graph [33]. Then, it assigns resource blocks to the nodes in order to satisfy requirement of their demanded slices in the descending order of their betweenness centrality, i.e. delay for URLLC slice and connectivity for mMTC slice;

3) *the Top-K solution*, which sequentially considers each type of slice, computes the total number of required resource blocks for satisfying requirement for each node, Λ_{sv}, and then assigns resource blocks for slice s in descending order of Λ_{sv} until exhausting available resource blocks or violating power constraint.

4) *Random method*, which randomly selects nodes and assigns resource blocks to them until exhausting available resource blocks or violating power constraint. Here, 100 cases were tested and the average result is noted.

All algorithms are implemented in MATLAB R-2020b. The performance of every solution is evaluated by the total power served after balancing the unbalanced test feeders in the distribution power system using optimal power flow model in section (II-A) for the given communication network, which is comprised of different slices as microwave links and sensors/actuators associated with power grid nodes. We show the percentage of the power served with respect to the case of secure and full connectivity between all nodes and the CC.

B. Simulation Setup

We evaluate the proposed solutions on the IEEE 13-, 34-, and 37-node test feeders [34], which represent simplified models of actual distribution circuits. These test feeders include unbalanced loading, switches, shunt capacitors and voltage regulators to compensate the severe voltage drops which caused by loaded transmission lines. Test feeders are shown in Fig. 3. In our simulations, we also insert different distributed generations in these test feeder models, such as rooftop solar PV systems. Table. III indicates the installation of distributed generations on particular buses in test feeders.

Table III: The bus location of installed distributed generations in the IEEE test feeders.

test feeder	installed DG
IEEE 13-node	684
IEEE 34-node	836, 842
IEEE 37-node	734, 727, 720

Calculation of power flow model, equations (1) and (2), were performed using CVX [35] integrated in MATLAB. The CC, which performs the power flow model, is situated on the highest degree nodes in the test feeders and communicates with other nodes. We assume that all communication nodes (including sensors, actuators, and relays) have battery backups and are hence cannot be affected by failures in the power grid.

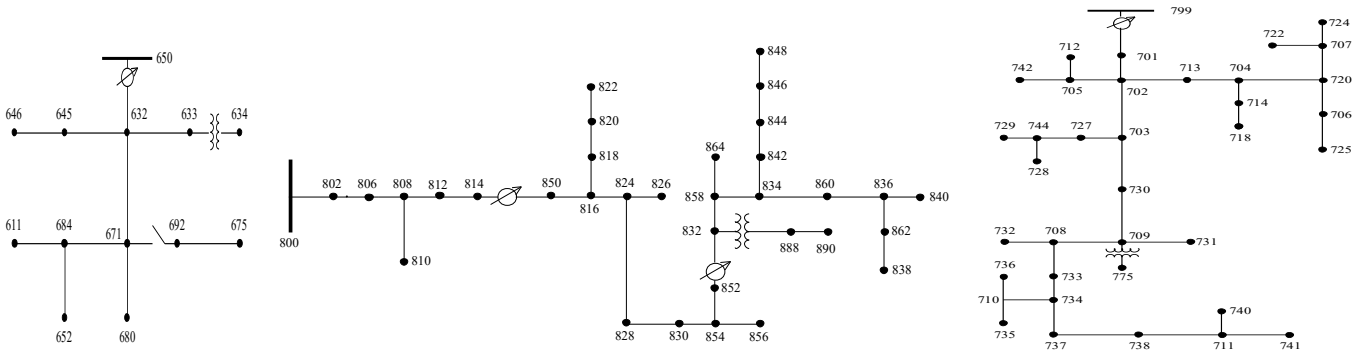

a) IEEE 13-node feeder b) IEEE 34-node feeder c) IEEE 37-node feeder

Figure 3: Different distribution test feeders.

The test feeders are mapped to an urban area while nodes are assigned to city blocks. In most cities, streets are typically laid out on a grid plan so that city blocks are square or rectangular. In this work, we consider a typical city block in Chicago which is 330 by 660 feet (100 m $\times$ 200 m) [36]. As we only consider line-of-site (LOS) transmissions, we assume antennas are placed on the roof of the blocks. We use homogeneous cells deployment and one gNB is considered for each cell in the center with radius 250 meter and maximum transmission power $P_{max} = 20$ W and $P = 30$ dBm. Each test feeder may be covered by multiple cells. We set small cell parameters based on [26]. .

We assumed a system bandwidth of $W = 20$ MHz with the carrier frequency 2 GHz. As we use FFR technique, the total bandwidth of each cell is divided between the inner zone and three outer zones. We assume that 2/3 of resources are assigned to the inner zone, and 1/9 of resources are assigned to each outer zone. The inner zone boundary is defined based on the path loss threshold, which is set to the path loss between the gNB and a node in the 2/3 radius of the cell. Furthermore, for the sake of simplicity, we assume only one MVNO exists in each cell with SLA equal to 1. The results can be simply extended to numerous MVNOs with different SLAs.

In this work, we suppose that all nodes require mMTC slice for the monitoring purpose, while URLLC slices are only needed by generators, switches, shunt capacitors, and regulators to receive the control command from the CC. D^s_{max}, the maximum tolerable delay for slice URLLC slice is set to 0.005 second [9]. Note that the number of required resource blocks to assign the needed slice varies depending on the channel gain between the gNB and nodes.

C. Results

This section first explains the settings used for the proposed greedy algorithm. Then, we compare all benchmarks together.

1) Setting Design Parameters:

Comparison under node weight definition:

Recalling that the priority of nodes, β_v, represents the importance of observing and controlling node v by the CC. We examine both the topological (the degree of the node in the power system topology) and the service (the injected power) importance of node v.

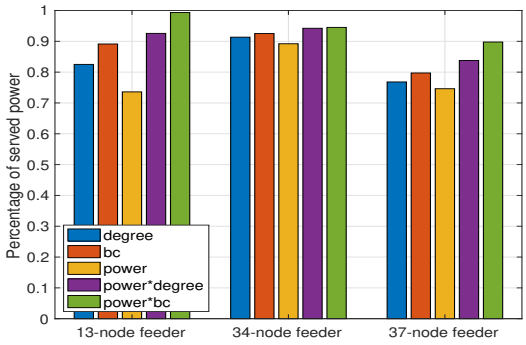

Figure 4: Performance evaluation under different node weights (β_v) for various test feeders in terms of served power after balancing the test feeders with respect to the case of secure and full connectivity between all nodes and the CC (slices are placed by the greedy heuristic under $|N| = 20$ and $\frac{\alpha_{s_U}}{\alpha_{s_M}} = 3$)

We compare performance of the greedy algorithm under five different definitions of weights: (i) degree, (ii) BC (Betwenness Centrality), (iii) power injection of nodes, (iv) power injection $\times$ degree, and (v) power injection $\times$ BC. The nodes' weights are normalized here. α_s for URLLC and mMTC slices are set to 3 and 1, respectively.

The results in Fig. 4 shows that the node weight definition of "the BC of the node $\times$ the real power injected at the node" attains the best performance for all test feeders as it considers both the topological (BC) and the service (power injection) importance of nodes. For the rest of the results in this section, we will use this definition of weight for the greedy heuristic.

Comparison under different slice importance:

Although monitoring the status and collecting data of various power grid nodes and sending relevant control signals are both critical in the proper operation of power systems, the controlling aspect has more fundamental importance. Nonetheless, SCADA, through dispatching control commands performs functions such as feeder voltage or VAR control, feeder automatic switching, etc. To the best of the authors' knowledge, there is no data to compare the importance level of controlling over monitoring action. Therefore, we compare performance of the greedy

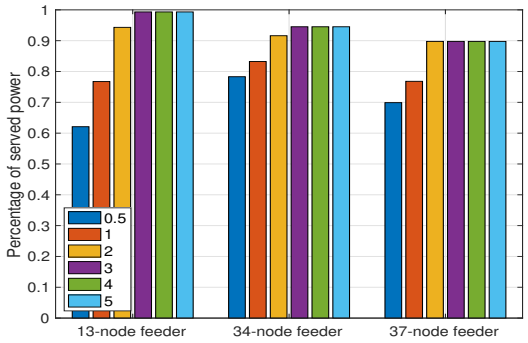

Figure 5: Performance evaluation under different importance of URLLC slice over mMTC slice ($\frac{\alpha_{s_U}}{\alpha_{s_M}}$) for various test feeders in terms of served demand after balancing the test feeders with respect to the case of secure and full connectivity between all nodes and the CC (slices are placed by the greedy heuristic under $|N| = 20$ and β_v = power injection $\times$ BC)

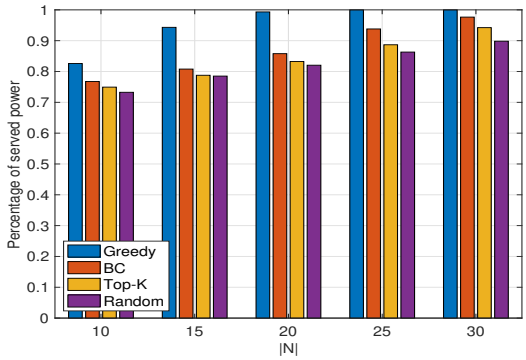

Figure 6: Performance evaluation under different number of resource blocks ($|N|$) for IEEE 13-node test feeder in terms of served demand after balancing the test feeders with respect to the case of secure and full connectivity between all nodes and the CC (for greedy heuristic under $\frac{\alpha_{s_U}}{\alpha_{s_M}} = 3$ and β_v = power injection $\times$ BC))

algorithm under different ratio of α_s for URLLC over mMTC slice.

In this scenario, we fix $\alpha_{s_M} = 1$ and change α_{s_U}. These values indicate α_s for mMTC and URLLC slices, respectively. As it can be seen, the performance improves considerably for larger amount of α_{s_U}, which shows the importance of controlling aspects of the SCADA network through dispatching control commands. The performance is almost completely insensitive to the $\alpha_{U_S} \geq 3$ for all test feeders. For the rest of the results in this section, we will use ($\frac{\alpha_{s_U}}{\alpha_{s_M}} = 3$) for the greedy heuristic.

2) Overall Comparison of All baselines:

Finally, Figs. 6-8 compare the performance of all algorithms in terms of served power in power grids after balancing different test feeders. Here, as the number of resource blocks increases, the control network delivers higher power. This is because more nodes are observable and controllable; hence the total served power improves. Moreover, results show that the greedy heuristic consistently exceeds all baselines, which emphasizes the importance of strategically placing slices considering system topology, generation/load contribution, and the importance of slices. The second best algorithm is the BC method, which prioritizes nodes with higher betweenness centrality. Intuitively, these nodes substantially influence other nodes in the radial distribution power grids. Next, the Top-K solution outperforms notably better than random benchmark. The results follow the same trend for all test feeders.

We also compare our results with the scenario of using Power Line Carrier Communication (PLCC) technology in the communication network when failures occur. PLCC links carry control communications over power lines. We start with a baseline where all links are PLCC. Then we impose a bus outages incident in the power grid. The affected PLCC links are are failed thus cutting off communications. The reason behind this realistic assumption is that outages are inevitable in the power grid, and while microwave links are immune to power grid failure, the loss of a power transmission line disables a PLCC link. Here, we impose initial bus outages of 5% and 10% of total nodes and after the cascade ends, we

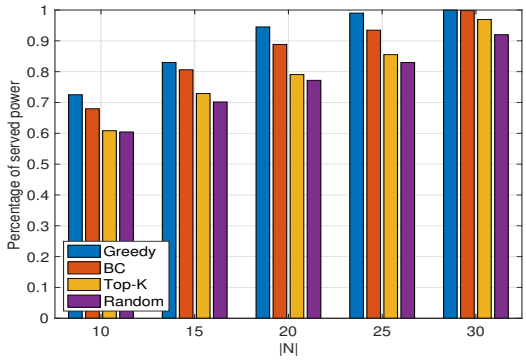

Figure 7: Performance evaluation under different number of resource blocks ($|N|$) for IEEE 34-node test feeder in terms of served demand after balancing the test feeders with respect to the case of secure and full connectivity between all nodes and the CC (for greedy heuristic under $\frac{\alpha_{s_U}}{\alpha_{s_M}} = 3$ and β_v = power injection $\times$ BC))

run the optimal power flow problem to balance test feeders. For each case, 100 random sets of node outages have been considered. By comparing the results in Table IV and Figs. 6-8, it is sensible that the proposed heuristic substantially provides higher served power which shows the importance of a secure communication network.

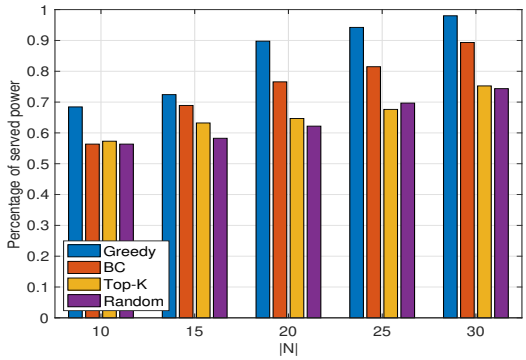

Figure 8: Performance evaluation under different number of resource blocks ($|N|$) for IEEE 37-node test feeder in terms of served demand after balancing the test feeders with respect to the case of secure and full connectivity between all nodes and the CC (for greedy heuristic under $\frac{\alpha_{s_U}}{\alpha_{s_M}} = 3$ and β_v = power injection $\times$ BC))

Table IV: The impact of initial bus outages in percentage of served power after balancing the test feeders (with respect to the case of secure and full connectivity between all nodes and the CC) in PLCC deployment on different the IEEE test feeders.

test feeder	5%	10%
IEEE 13-node	68.945	52.865
IEEE 34-node	73.738	54.279
IEEE 37-node	71.912	44.539

V. Conclusion & Future Work

This paper helps to clarify the challenges and trends of RAN network slicing and advances the practicality of using network slicing technology in the distribution power grid.

5G Network slicing saves bandwidth and reduces latency, and meets the ultra-low latency requirement of millisecond-level control services on the power grid.

In this work, we look at the bandwidth allocation in Radio Access Network (RAN) 5G-NR network slicing to maximize spectral efficiency, subject to providing each sensor and actuator in the power grid a guaranteed minimum requirement of slices. We not only proved the NP-hardness of the proposed solution, but we also developed a greedy heuristic to solve the problem quickly. Extensive simulations on the IEEE 13-, 34-, and 37-node test feeder showed that the proposed algorithm achieves efficacy in total power served after balancing the unbalanced power grid.

References

[1] C. Field, V. Barros, K. Mach, and M. Mastrandrea, *Climate change 2014: impacts, adaptation, and vulnerability – IPCC WGII AR5 summary for policymakers*, 01 2014, pp. 1–32.

[2] P.-J. Alet, F. Baccaro, M. De Felice, V. Efthymiou, C. Mayr, G. Graditi, M. Juel, D. Moser, M. Petitta, S. Tselepis, and G. Yang, "Quantification, challenges and outlook of pv integration in the power system: a review by the european pv technology platform," in *Proceedings of EU PVSEC*, 2015, eU PVSEC 2015 ; Conference date: 14-09-2015 Through 18-09-2015.

[3] C. T. SGCC and Huawei, "Powered by sa: Smart grid 5g network slicing," 3 2020.

[4] X. xia, L. Zhang, C. Mei, J. Li, x. Zhu, Y. Liang, and J. Song, "A survey on 5g network slicing enabling the smart grid," 12 2019, pp. 911–916.

[5] E. P. S. A. . O. Software, "System optimization," https://etap.com/packages/system-optimization.

[6] Ericsson.com/industrylab. (March, 2020) Bringing 5g to power, opportunities and challenges with connected power distribution grids.

[7] J. Ordonez-Lucena, O. Adamuz-Hinojosa, P. Ameigeiras, P. Muñoz, J. J. Ramos-Muñoz, J. F. Chavarria, and D. Lopez, "The creation phase in network slicing: From a service order to an operative network slice," in *2018 European Conference on Networks and Communications (EuCNC)*, 2018, pp. 1–36.

[8] K. Boutiba, A. Ksentini, B. Brik, Y. Challal, and A. Balla, "Nrflex: Enforcing network slicing in 5g new radio," *Computer Communications*, vol. 181, 10 2021.

[9] T. Ma, Y. Zhang, F. Wang, D. Wang, and D. Guo, "Slicing resource allocation for embb and urllc in 5g ran," *Wireless Communications and Mobile Computing*, vol. 2020, pp. 1–11, 01 2020.

[10] A. A. Gebremariam, T. Bao, D. Siracusa, T. Rasheed, F. Granelli, and L. Goratti, "Dynamic strict fractional frequency reuse for software-defined 5g networks," in *2016 IEEE International Conference on Communications (ICC)*, 2016, pp. 1–6.

[11] S. O. Oladejo and O. E. Falowo, "Latency-aware dynamic resource allocation scheme for multi-tier 5g network: A network slicing-multitenancy scenario," *IEEE Access*, vol. 8, pp. 74 834–74 852, 2020.

[12] K. Zhu and E. Hossain, "Virtualization of 5g cellular networks as a hierarchical combinatorial auction," *IEEE Transactions on Mobile Computing*, vol. 15, no. 10, pp. 2640–2654, 2016.

[13] M. Richart, J. Baliosian, J. Serrat, and J.-L. Gorricho, "Resource slicing in virtual wireless networks: A survey," *IEEE Transactions on Network and Service Management*, vol. 13, no. 3, pp. 462–476, 2016.

[14] S. R. Pokhrel, J. Ding, J. Park, O.-S. Park, and J. Choi, "Towards enabling critical mmtc: A review of urllc within mmtc," *IEEE Access*, vol. 8, pp. 131 796–131 813, 2020.

[15] A. Anand, G. de Veciana, and S. Shakkottai, "Joint scheduling of urllc and embb traffic in 5g wireless networks," *IEEE/ACM Transactions on Networking*, vol. 28, no. 2, pp. 477–490, 2020.

[16] M. Alsenwi, N. H. Tran, M. Bennis, A. Kumar Bairagi, and C. S. Hong, "embb-urllc resource slicing: A risk-sensitive approach," *IEEE Communications Letters*, vol. 23, no. 4, pp. 740–743, 2019.

[17] M. Alsenwi, N. H. Tran, M. Bennis, S. R. Pandey, A. K. Bairagi, and C. S. Hong, "Intelligent resource slicing for embb and urllc coexistence in 5g and beyond: A deep reinforcement learning based approach," *IEEE Transactions on Wireless Communications*, vol. 20, no. 7, pp. 4585–4600, 2021.

[18] A. Pradhan and S. Das, "Joint preference metric for efficient resource allocation in co-existence of embb and urllc," in *2020 International Conference on COMmunication Systems NETworkS (COMSNETS)*, 2020, pp. 897–899.

[19] G. Sun, K. Xiong, G. O. Boateng, D. Ayepah-Mensah, G. Liu, and W. Jiang, "Autonomous resource provisioning and resource customization for mixed traffics in virtualized radio access network," *IEEE Systems Journal*, vol. 13, no. 3, pp. 2454–2465, 2019.

[20] Q. Ye, W. Zhuang, S. Zhang, A.-L. Jin, X. Shen, and X. Li, "Dynamic radio resource slicing for a two-tier heterogeneous wireless network," *IEEE Transactions on Vehicular Technology*, vol. 67, no. 10, pp. 9896–9910, 2018.

[21] P. Popovski, K. F. Trillingsgaard, O. Simeone, and G. Durisi, "5g wireless network slicing for embb, urllc, and mmtc: A communication-theoretic view," *IEEE Access*, vol. 6, pp. 55 765–55 779, 2018.

[22] H.-T. Chien, Y.-D. Lin, C.-L. Lai, and C.-T. Wang, "End-to-end slicing as a service with computing and communication resource allocation for multi-tenant 5g systems," *IEEE Wireless Communications*, vol. 26, no. 5, pp. 104–112, 2019.

[23] X. Foukas, G. Patounas, A. Elmokashfi, and M. K. Marina, "Network slicing in 5g: Survey and challenges," *IEEE Communications Magazine*, vol. 55, no. 5, pp. 94–100, 2017.

[24] C. Campolo, A. Molinaro, A. Iera, and F. Menichella, "5g network slicing for vehicle-to-everything services," *IEEE Wireless Communications*, vol. 24, pp. 38–45, 12 2017.

[25] K. Samdanis, X. Costa-Perez, and V. Sciancalepore, "From network sharing to multi-tenancy: The 5g network slice broker," *IEEE Communications Magazine*, vol. 54, no. 7, pp. 32–39, 2016.

[26] S. O. Oladejo and O. E. Falowo, "5g network slicing: A multi-tenancy scenario," in *2017 Global Wireless Summit (GWS)*, 2017, pp. 88–92.

[27] W. Kersting, *Distribution System Modeling and Analysis*, 02 2016.

[28] L. Gan and S. H. Low, "Convex relaxations and linear approximation for optimal power flow in multiphase radial networks," in *2014 Power Systems Computation Conference*, 2014, pp. 1–9.

[29] M. B. Cain, R. P. O'neill, and A. Castillo, "History of optimal power flow and formulations optimal power flow," 2012.

[30] Z. Wang, D. S. Kirschen, and B. Zhang, "Accurate semidefinite programming models for optimal power flow in distribution systems," 2017.

[31] N. Al-Falahy and O. Y. K. Alani, "Network capacity optimisation in millimetre wave band using fractional frequency reuse," *IEEE Access*, vol. 6, pp. 10 924–10 932, 2018.

[32] F. Kelly, "Charging and rate control for elastic traffic," *European Transactions on Telecommunications*, vol. 8, 02 1997.

[33] J. Golbeck, "Chapter 21 - analyzing networks," in *Introduction to Social Media Investigation*, J. Golbeck, Ed. Boston: Syngress, 2015, pp. 221 – 235. [Online]. Available: http://www.sciencedirect.com/science/article/pii/B9780128016565000214

[34] K. P. Schneider, B. A. Mather, B. C. Pal, C.-W. Ten, G. J. Shirek, H. Zhu, J. C. Fuller, J. L. R. Pereira, L. F. Ochoa, L. R. de Araujo, R. C. Dugan, S. Matthias, S. Paudyal, T. E. McDermott, and W. Kersting, "Analytic considerations and design basis for the ieee distribution test feeders," *IEEE Transactions on Power Systems*, vol. 33, no. 3, pp. 3181–3188, 2018.

[35] M. Grant and S. Boyd, "CVX: Matlab software for disciplined convex programming, version 2.1," http://cvxr.com/cvx, Mar. 2014.

[36] C. D. of Transportation, "Street and site plan design standards," April 2007. [Online]. Available: https://www.chicago.gov/dam/city/depts/cdot/StreetandSitePlanDesignStandards407.pdf